

Chapter 1

Perceptual Thumbnail Generation

WEI FENG #1

School of Computer Science and Technology
Tianjin University
Tianjin, P.R. China
Email: wfeng@tju.edu.cn

LIANG WAN #2

School of Computer Software
Tianjin University
Tianjin, P.R. China
Email: lwan@tju.edu.cn

ZHOUCHE LIN #3

Microsoft Research Asia
Beijing, P.R. China
Email: zhoulin@microsoft.com

TIEN-TSIN WONG #4

Dept of Computer Science & Engineering
The Chinese University of Hong Kong
Hong Kong, P.R. China
Email: ttwong@cse.cuhk.edu.hk

ZHI-QIANG LIU #5

School of Creative Media

City University of Hong Kong

Hong Kong, P.R. China

Email: zq.liu@cityu.edu.hk

1.1 Introduction

As shrunk versions of pictures, thumbnails are commonly used in image preview, organization, and retrieval [1], [2], [3], [4]. In the age of digital media, a thumbnail plays quite similar role for an image as an abstract does for an article. Through a thumbnail, viewers expect to observe both the global composition and important perceptual features of the original full-size picture, thus to obtain a faithful impression about the image content and quality by inspecting the thumbnail only.

In practice, thumbnails mainly serve in the following two aspects. First, they provide viewers a convenient way to preview high-resolution pictures on a small display screen. For instance, many portable devices, e.g., digital cameras and cell phones, provide prompt image preview function by small-size LCD displays [5], as shown in Figure 1.1. Second, thumbnails enable users to quickly browse a large number of images without being distracted by unimportant details. For example, almost all visual search engines, such as Google Images and Bing Images, use thumbnails to organize their returned search results. As the proliferation of digital images in recent years, how to generate perceptually faithful thumbnails become a crucial problem.

From the historical viewpoint, the concept of thumbnail is gradually changed due to the developing practical requirements in real-world applications. At the very beginning, for a given full-size picture, a thumbnail was generated simply by filtering and subsampling [6], [7]. Then, to emphasize some important portions in original pictures, ROI-based thumbnails were proposed based on visual attention models [1], [8]. Compared to conventional downsampled thumbnails that equally treat all image parts and features in the original size, ROI-based thumbnails highlight visually important regions only, thus helping viewers to focus on essential parts, but inevitably losing the perceptual faith of global composition in original pictures. In recent years, moreover, people start to realize the necessity and importance of *perceptual thumbnails* [5], [9]. Specifically, perceptual thumbnails highlight the quality-related and perceptually important features in original pictures, with the global structural composition preserved. From perceptual thumbnails, viewers can easily assess the



Figure 1.1: Examples of image preview approaches. (a) Looking at the printed photograph. (b) Preview in the LCD display screen of a digital camera. Note that, the size of region γ_b in (b) is much smaller than its corresponding region γ_a in (a), thus the perception-related features are less noticeable. When the resolution of γ_b is below some threshold, viewers cannot clearly perceive the phenomena occurring in the region using preview approach (b).

image quality without checking the original full-size versions, thus facilitating faithful image preview on small displays and fast browsing of a large number of pictures. In contrast, without perceptual thumbnails, when users want to evaluate the quality of images taken by digital cameras (see Figure 1.1 for example), they have to repeatedly zoom in, zoom out at different scales, and shift across different parts of the images at higher resolutions, which is very time consuming, inconvenient and ineffective. Moreover, the operation of zooming in may also make viewers losing the perception of the global composition of images.

Clearly, both conventional downsampled thumbnails and ROI-based thumbnails are not qualified to serve as perceptual thumbnails. As shown in Figure 1.2, some apparent perceptual features in the original pictures, e.g., blur and noise, may easily be lost in the downsampled thumbnails, no matter what interpolation algorithm is used, the reason of which is two-fold. First, to discover a phenomenon in an image, the resolution of the phenomenon must be larger than some threshold that represents the perceiving capability of viewers. Second, the conventional downsampling process may significantly reduce the resolution of perceptual features in downsampled thumbnails. When the reduced resolution of naively downsampled perceptual features become less than viewers' perceiving thresholds, these features cannot be noticed. See Figure 1.1(a) and (b) for an illustration. As a result, in perceptual thumbnails, some important quality-related features should be highlighted, i.e., to preserve the resolution of perceptual features from the downsampling process. Besides, it is easy to understand why ROI-based thumbnails (see Figure 1.3) cannot be used as perceptual thumbnails, as they destroy the global composition of the original pictures.

In particular, successful perceptual thumbnail generation should meet the following four requirements.

- Low cost: As thumbnails are widely used in prompt preview of high-resolution pictures and fast

browsing of a large number of images, they must be generated in a computation and storage economic way. Hence, fast and simple algorithms for highlighting perceptual features are desirable.

- **Unsupervision:** Since we may want to quickly produce a large number of thumbnails in a browsing task, they should be generated automatically. Both preliminary training and on-the-fly parameters tuning should be avoided.
- **Highlighting multiple perceptual features:** To faithfully reflect the content and quality of original full-size pictures in thumbnails, multiple quality-related features, such as blur and noise, should be highlighted according to their respective degrees.
- **Preserving the original composition:** It is important for perceptual thumbnails to provide viewers with a clear impression about the global structure of original pictures. For instance, users may want to quickly decide whether or not to take a second shot on the same scene by checking the thumbnails on small display screens in their cameras. Thus, it is better to preserve the original composition in perceptual thumbnails.

In this chapter, we focus on introducing the recent development of perceptual thumbnail generation techniques that satisfy the above four requirements. Within a unified framework, we pay our particular attention to preserving and highlighting two types of quality-related perceptual features, i.e., blur and noise.

This chapter begins with Section 1.2 that briefly introduces the techniques for traditional thumbnail generation. We specifically discuss signal-level downsampled thumbnail generation and ROI-based thumbnail generation methods. Signal-level thumbnail generation focuses on the development of different filtering or interpolation techniques so as to reduce the aliasing artifacts in thumbnails. In contrast, ROI-based thumbnail generation aims to preserve salient image regions and essential structures during image resizing. The trend, pros and cons of each method are also discussed.

The next three sections present the technical details of this chapter. Specifically, in Section 1.3, we first describe the commonly noticed visual cues/features that indicate image quality and need to be preserved in perceptual thumbnails. Then, a general framework for perceptual thumbnail generation is presented, which focuses on two types of low-level perceptual features, blur and noise, and can be easily extended to include other types of perceptual features, such as bloom and overexposure. The two features, blur and noise, are most commonly encountered in digital photography and can degrade the quality of pictures significantly. At last, we briefly introduce several state-of-the-art perceptual thumbnail generation methods that are based on the proposed general working flow. From Section 1.4 to Section 1.5, we elaborate how to highlight spatially variant blur and homogeneous noise in thumbnails, respectively. Although blur and noise estimation has been studied for decades in image processing and computer vision, most previous deblurring and denoising

methods tried to get an accurate estimate of blur and noise strength for the goal of recovering blur-free and noise-free images. Perceptual thumbnail generation, on the contrary, aims to highlight blur and noise at a noticeable scale in thumbnails. This raises the requirements of fast, appropriate but inexact algorithms for blur and noise estimation, as well as alias-free blur and noise visualization. For this purpose, we discuss in depth how to quickly estimate blur and noise from the original images, and effectively visualize them in the downsampled thumbnails.

In Section 1.6, we present a number of experimental results that comprehensively compare the performance of different techniques in perceptual thumbnail generation. Current perceptual thumbnail generation only handles blur and noise, the two low-level visual cues. After summarizing the state-of-the-arts of perceptual thumbnail generation in Section 1.7, we discuss some possible ways to highlight other types of perceptual cues, including red-eye effect and bloom, in thumbnails.

1.2 Traditional Thumbnail Generation

Traditional thumbnail generation techniques can be classified into two categories, signal-level thumbnail generation and ROI-based thumbnail generation. Signal-level thumbnail generation techniques [10], [11], [12], [13], [7] create the thumbnail from a high-resolution original image by prefiltering and subsampling. The generated thumbnail preserves the original composition. ROI-based thumbnail generation techniques [3], [2], [14], [15], [16], on the other hand, aim at detecting and retaining important regions in the resulting thumbnail. In the following two subsections, we will introduce the traditional thumbnail generation techniques in detail.

1.2.1 Signal-level thumbnail generation

Signal-level thumbnail generation relies on image resampling techniques, which usually consist of two components, filtering and subsampling [17]. Due to different filtering schemes employed, the quality of the resulting thumbnails may differ greatly. Among the existing image resampling techniques, the simplest method is decimation, i.e. keeping some pixels of the original image and throwing others away. Without prefiltering the original image, decimation typically leads to significant aliasing artifacts, as shown in Figure 1.2(b).

To reduce such aliasing artifacts, low-pass filters can be used before decimation. For example, box filter computes an average of pixel values within the pixel neighborhood. Bilinear filter performs linear filtering first in one direction, and again in the other direction. Bicubic filter [10] is often chosen over bilinear filter since the resampled image is smoother and has fewer aliasing artifacts. Other than second-order polynomials defined in bilinear filter and third-order polynomials defined in bicubic filter, high order

piecewise polynomials [12] can also be used, although the improvement is marginal. More sophisticated B-spline approximation is reported in the literature for image resampling [11], [7]. Other linear filters are also known, including Lanczos [6] and Mitchell [18]. The aforementioned filters are space-invariant (isotropic) in nature. In the context of texture mapping, perspective mapping leads to space-variant (anisotropic) footprint. For this application, elliptic Gaussian-like filters have been employed [19], [20], [21].

Another trend of image resampling is to perform edge-adaptive interpolation so as to generate sharp edges in the resampled image. Li and Orchard [22] developed an edge-directed image interpolation (NEDI) algorithm. They estimated local covariance from a low-resolution image and used the low-resolution covariance to adapt the image interpolation at a higher resolution. Muresan and Parks [23] developed a method to optimally determine the local quadratic signal class for the image. Zhang and Wu [24] proposed an edge-guided non-linear interpolation algorithm, which estimates two observation sets in two orthogonal directions, and then fuses the two observation sets by the linear minimum mean square-error estimation technique. Fattal [25] relied on a statistical edge dependency relating edge features of two different resolutions, and solved a constrained optimization. It should be noted that edge-adaptive resampling techniques are specially designed for image upsampling, and they are usually not suitable for image downsampling.

Figure 1.2 illustrates several commonly-used image resampling methods. The original image has a resolution of 2048×1536 , and is downsampled to a resolution of 320×240 . As shown in Figure 1.2(d), decimation results in severe aliasing artifacts. Bilinear filtering, shown in Figure 1.2(e), removes artifacts. Bicubic filtering, shown in Figure 1.2(f), produces a smoother thumbnail by further reducing the aliasing artifacts. The thumbnail due to Lanczos filtering, shown in Figure 1.2(g), has less artifacts, although this filtering is much slower than others. Obviously, signal-level thumbnail generation techniques can prevent aliasing artifacts and preserve the original image composition. However, they are not designed to preserve perceptual image quality during image resampling. In fact, they probably lose such features that are useful to users to identify the image quality. Look at the blowups in Figures 1.2(b) and (c). The original high-resolution image suffers to noticeable blur and noise. However, the four thumbnails all appear rather clean and clear. A qualitative analysis of the loss in the blur and noise will be presented in Section 1.3.

1.2.2 ROI-based thumbnail generation

Unlike signal-level thumbnail generation which preserves the original image composition, ROI-based thumbnail generation just displays important image regions in the small-scale thumbnail. Burton et al. [1] tried to generate thumbnails that could be recognized more quickly. They reduced the downsampling distortion by treating the high-resolution original image with edge-preserving smoothing, lossy image compression or static codebook compression. Chen et al. [8] incorporated user attention to adapt the high-resolution

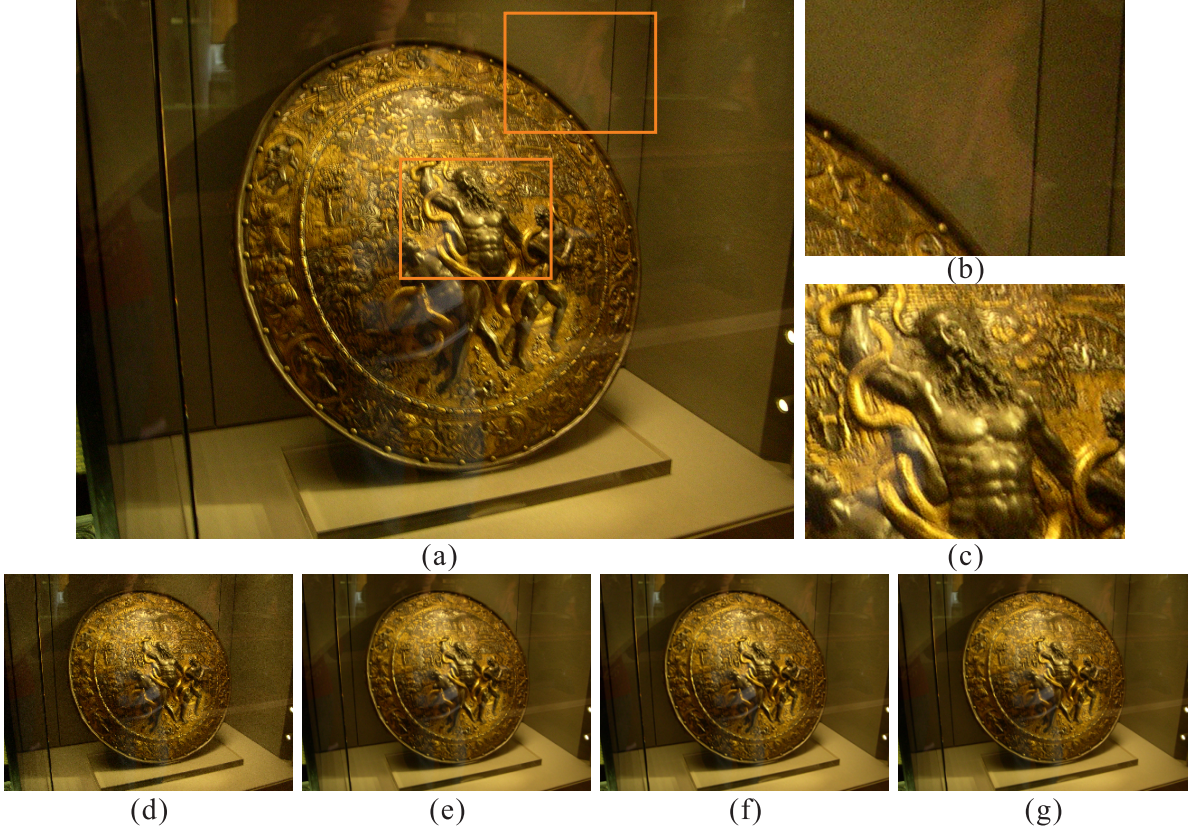


Figure 1.2: Signal-level thumbnail generation. (a) The original image has a resolution of 2048×1536 , and is downsampled to a resolution of 320×240 . Two blowups are shown in (b) and (c). Thumbnails are downsampled using (d) decimation, (e) bilinear, (f) bicubic and (g) Lanczos filtering.

image on small-size screens. They defined an image attention model based on region of interest, attention value and minimal perceptible size. For screens with different scale and aspect ratio, different important regions are cut out of the original image for downsampling. Similarly, Suh et al. [14] detected key components of the high-resolution image based on a saliency map, and then cropped images prior to downsampling. Figure 1.3(a) illustrates this idea. Although the cropping-based methods can render important image portions more recognizable, users will lose the global overview of the original image.

Another research direction relating to thumbnail generation is image retargeting, which considers geometric constraints and the image content as well during image resizing. Setlur [26] aimed to maximize salient image objects by minimizing less important image portions in-between. Since the spatial spaces between image objects may be narrowed, the relative geometric relation between the objects can be altered in the thumbnail. Avidan and Shamir [15] presented a seaming carving approach, which removes or inserts an 8-connected path of pixels on an image from top to bottom, or from left to right in one pass. This method, though quite simple, is rather time consuming and may damage the image structure severely. One example is shown in Figure 1.3(b). To address the problems in seaming carving, a series of retargeting techniques [16],



Figure 1.3: ROI-based thumbnail generation for the high-resolution image in Figure 1.17(a). (a) Automatical cropping [14]. (b) Seam carving [15].

[27], [28], [29] have been proposed. Although the techniques can be quite different, their objectives are similar, including preserving the important image content, reducing visual artifacts, and preserving internal image structures. A comprehensive evaluation of state-of-art methods can be found in Reference [30].

In addition, special concerns have been reported to address the situation when there are texts in the high-resolution image. For example, Woodruff et al. [3] created thumbnails for Web pages by combining text summaries and image thumbnails. Berkner et al. [2] cropped and scaled image and text segments from the original image, and generated a more readable layout for a particular display size. Following the aforementioned two works, many subsequent research works can be found, including [31], [32], [33].

These ROI-based thumbnail generation techniques have been proven successful in preserving the important image content in the low-resolution thumbnail. However, none of them accounts for perceptual quality features in the high-resolution image. As a result, they may remove features that indicate whether the image is well shot during image downsizing.

1.3 Perceptual Thumbnail Generation

In this section, we first describe several commonly noticed visual/perceptual cues in images that are quality indicative. In the next, we present a general framework for perceptual thumbnail generation, with specific focus on highlighting blur and noise in thumbnails. We end this section by a brief overview of the state-of-the-art methods in perceptual thumbnail generation.

1.3.1 Quality-indicative visual cues

Given a picture shot with a digital camera, users often have a demand to inspect whether or not the picture is well shot by quickly checking the thumbnail image only. Properly highlighting some perceptual features in the thumbnail may certainly benefit such quality inspection process. However, to realize this target, we

first need to find what features or effects in the original picture should be highlighted in the thumbnail. According to practical photography experiences, we find that there are generally two categories of quality-related perceptual features, i.e., low-level image features, and high-level semantic features, which will be introduced in the following at length.

Low-level image features There are some features that degrade the quality of an image but have less to do with the image content, including blur, noise, bloom, overexposure and underexposure etc. In most cases, these features are quality indicative and should be noticed by users during their photo taking process, thus should be preserved and highlighted from the downsampling operation in thumbnails. In the following, we describe in detail about these quality-related low-level perceptual features.

- **Blur:** Except for some special cases, a blurry picture is usually inferior to a sharp picture of the same scene, especially when the blur is caused by unexpected reasons, such as hand shaking. In most cases, if we inspect unexpected blur in a picture through the preview screen of digital cameras, we may choose to take a second shot on the same scene. Hence, blur is a very important quality-indicative effect in images. In practice, accidental blur is almost inevitable for most unprofessional users. For example, users often accidentally move their hands during photo shooting. Besides, blur may also occur when there are moving objects in the scene or when some subjects are out of focus of the camera. Image blur caused by different reasons may exhibit different spatial properties, including spatial-varying blur and homogeneous blur. No matter caused by what reasons, image blur certainly should be highlighted in perceptual thumbnails. An example of image blur is shown in Figure 1.4(a).
- **Noise:** Image noise is the random variation of color or brightness information produced by image sensors during exposure and A/D conversion. It often looks like color grains and scatters over the entire image. There are two types of image noise, fixed noise and random noise [34]. Fixed noise is generally visible when using long exposure time or when shooting under low light conditions with high ISO. It has the same pattern under similar lighting conditions. Random noise occurs at all exposure times and light levels. It appears as randomly fluctuated intensities and colors, and will be different even under the identical lighting condition. Banding noise is a special type of random noise that appears as horizontal or vertical strikes. It is generated by the camera when reading data from image sensors, and is more noticeable at high ISO speed. Generally, noise will degrade the quality of a picture, thus is also quality-indicative. Figure 1.4(b) demonstrates how image noise appears in a picture.
- **Bloom:** Bloom is the phenomenon that a bright light source appears as a bright halo and leads to color bleeding into nearby objects. This phenomenon occurs when the light source is so strong that the

sensor pixels become saturated. For example in Figure 1.4(c), shooting direct sunlight will generate such effect around the boundary of sunlight area. The appearance of bloom will significantly destroy the local details of a scene, thus is quality-indicative.

- Overexposure and underexposure: Overexposure and underexposure refer to the effect of losing details in highlight and shadow regions, respectively. They are usually caused by inappropriate setting of camera's shutter speed and exposure. In high-resolution photography, except for some special effects, overexposure and underexposure may degrade the image quality in details, thus should be avoided.

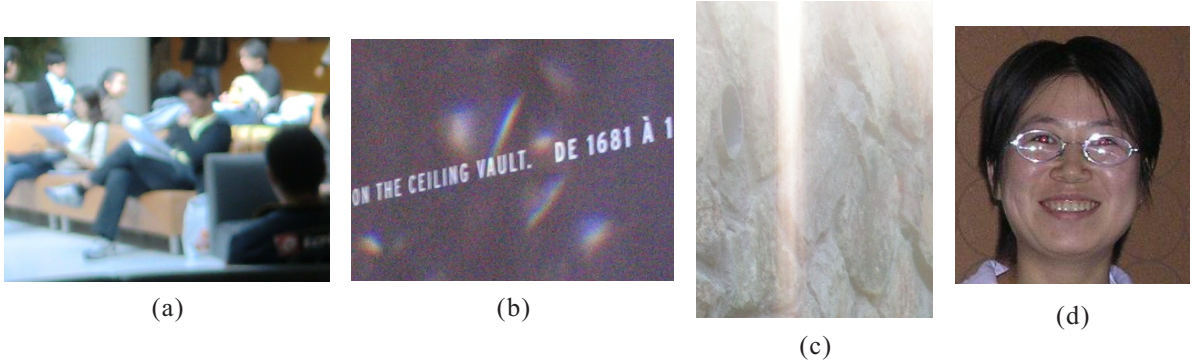


Figure 1.4: Quality-indicating visual cues. (a) Blur. (b) Noise. (c) Bloom. (d) Defected eyes.

High-level semantic features High-level perceptual features are highly related to image content [35], either reflects some unexpected phenomena of the particular objects, or even relates to some aesthetic aspects of the image. Some typical high-level perceptual features are listed below. High-level perceptual features are more difficult to be detected and highlighted in thumbnails than low-level perceptual features.

- Defected eyes: When shooting a picture of a group of people, users always care about whether his/her eyes are closed, or appear in red due to reflected flash. The Half-/closed eye effect often appears in the case that one person happens to close his/her eyes when the shutter is pressed. The red-eye effect is caused when users shoot a portrait picture in a dark room using a flash (as shown in Figure 1.4(d)). In the literature, different techniques [36], [37] have been developed to automatically detect and correct the red eyes.
- Simplicity: The most discriminative factor that differentiates professionals from amateur photographers is whether the photo is simple [35]. For a picture, being simple means it is easy to separate the subject from the background. There are various ways for professionals to achieve this goal, including making background out of focus, choosing significant color contrast, and using large lighting contrast

between the subject and the background. Recently, simplicity was also used as an important criterion for image quality assessment [35].

- Realism: Similar to simplicity, realism is another high-level feature that reflects aesthetic image quality [35]. Professional photographers often carefully choose the lighting conditions and the color distribution, and make use of filters to enhance the color difference. They are also very deliberate in the picture composition of the subject and background. All these are for the purpose of keeping the foreground of pictures as realistic as possible.

In the context of thumbnail generation, some features (e.g., simplicity and realism) might remain in the low-resolution thumbnail to some extent, while other features (e.g., blur, noise, bloom, overexposure, underexposure, defected eyes) are less noticeable due to the downsampling process. In this chapter, we will focus on studying how to preserve two typical low-level image features, i.e., blur and noise, in thumbnails. Note that, blur and noise may significantly degrade image quality and commonly exist in digital pictures.

1.3.2 A general framework

Before presenting the general framework of producing perceptual thumbnails, we first qualitatively analyze the reason that causes the loss of blur and noise features by conventional image downsampling. Suppose the original image is represented as vector x . Denote the antialiasing low-pass filter as T , and denote subsampling operation as S . The conventional thumbnail can then be expressed as

$$y = S \circ T(x), \quad (1.1)$$

where \circ stands for function composition. When the original image suffers from blur and noise, it can be formulated as

$$x = B(\hat{x}) + n, \quad (1.2)$$

where B and n represent the blur and noise, respectively, and \hat{x} is the ideal image without blur and noise degradation. By substituting Equation 1.2 into Equation 1.1, we get

$$y = S \circ T \circ B(\hat{x}) + S \circ T(n). \quad (1.3)$$

Let us examine the first term $S \circ T \circ B(\hat{x})$. Except for some extreme blurs, the low-pass filter B , usually representing accidental blur, has a much larger bandwidth than the low-pass filter T . In other words, compared to the influence of filter T , the influence of filter B can be much less noticeable in small-resolution thumbnails. Consequently, the conventional downsampled thumbnails will appear rather sharp than at their original scales.

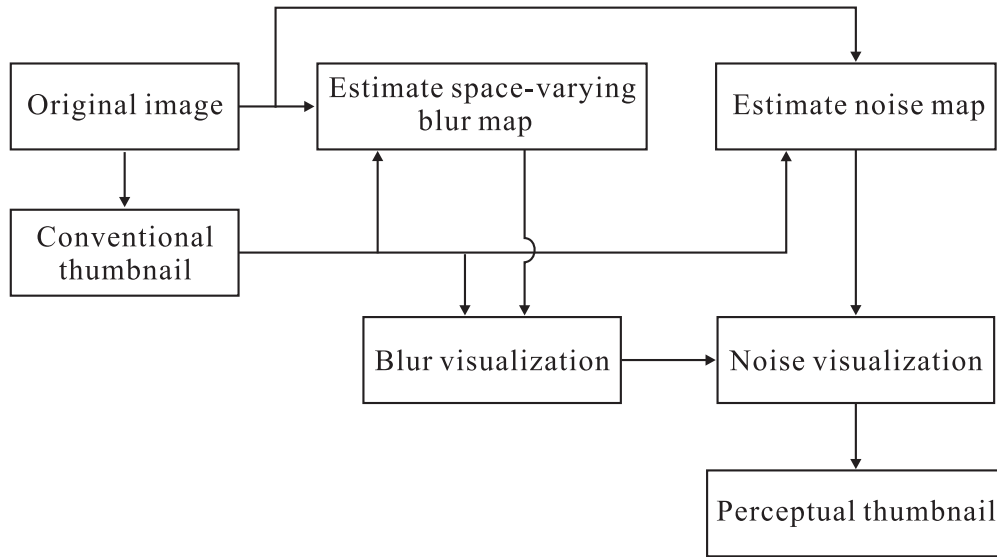


Figure 1.5: The framework of perceptual thumbnail generation, which particularly highlights two typical perceptual features, i.e., blur and noise. This framework uses the general extract-and-superimpose strategy that can be easily extended to include other types of perceptual features.

Now let us consider the second term in Equation 1.3. The noise n , mostly composed of lots of high frequency information, is filtered by T , thus will become much less apparent than in the original resolution. For instance, if n is a Gaussian noise of zero mean and moderate variance, $T(n)$ will be close to 0 under typical downsampling factors. As a result, the conventional thumbnail y will appear rather clean.

To highlight the blur and noise effects in y with proper strength, we can formulate the perceptual thumbnail as

$$y' = B(y) + n. \quad (1.4)$$

Intuitively, we further blur the conventional thumbnail according to the blur strength in the original image, and superimpose the noise information at the same time. By this way, users can easily inspect and discover the blur and noise level in the image by viewing the thumbnail alone.

Using the above *extract-and-superimpose* strategy, we can now summarize the general framework of perceptual thumbnail generation, which is capable of highlighting blur and noise features. As illustrated in Figure 1.5, we first downsample the high-resolution image and get the conventional thumbnail. We then estimate and extract the blur and noise information presented in the original high-resolution image. Afterwards, the detected amount of blur is properly added into the thumbnail, followed by rendering the estimated noise. We finally get the refined perceptual thumbnail. Note that, the presented framework for perceptual thumbnail generation is general enough and can be easily extended to include other types of perceptual features.

1.3.3 State-of-the-art methods

Although perceptual thumbnail generation is relatively a new topic, there are several related preliminary works that have been reported in the literature. For instance, the image preview method we introduced in [5] divides the problem of perceptual thumbnail generation into two tasks, i.e., structure enhancement and perceptual feature visualization. The first task highlights the salient structure and suppresses the subtle details in the image by non-linearly modulating the image gradient field. The second task estimates the strength of blur and noise in the original image and then superimposes blur and noise with appropriate degrees in the conventional thumbnail. Similarly, Samadani et al. [4] also studied how to estimate and visualize blur and noise features in the thumbnail. They generated the perceptual thumbnail by directly blurring the conventional thumbnail and adding noise to it. Besides, they further improved the noise estimation method to achieve a fast performance [9]. In addition, other related efforts in this direction have been exploited by Yamany [38] and Trentacoste et al. [39].

Current perceptual thumbnail generation is highly related to the problems of image deblurring [40], [41], [42] and denoising [43], [44]. These two problems are rather difficult, and the relevant algorithms are usually complicated and time-consuming. In contrast, instead of reconstructing the ideal high-resolution image, the goal of perceptual thumbnail generation is to visualize blur and noise in a proper way with reasonable complexity. This relieves the need of recovering actual blur kernels and estimating the noise accurately. Instead, a rough yet fast algorithm for blur and noise estimation is preferable. This is indeed what the existing works of perceptual thumbnail generation are mainly focused on. Although most existing works consider blur and noise in perceptual thumbnails, they adopt quite different algorithms for blur/noise estimation and rendering. In the reminder of this chapter, we will introduce in details the two representative methods proposed in [5] and [4].

1.4 Highlight Blur in Thumbnails

This section introduces how to highlight the reduced blurriness in perceptual thumbnails. Specifically, for the blurred regions in original high-resolution pictures, perceptual blur highlight is to magnify the reduced blurriness in their downsampled counterparts; while for the sharp regions at original scales, perceptual blur highlight maintains their clearance in thumbnails. Hence, there are two major steps in perceptual blur highlight, i.e., blur strength extraction from the original pictures, and faithful visualization of extracted blurriness in thumbnails.

1.4.1 Blur estimation

In the literature, there are many existing methods for blur estimation, providing global blur metrics and evaluating the overall blurriness of an image [45], [46], [47]. A suitable global blur metric is helpful to assess images with uniform blurs, such as the motion blur due to shaking cameras. It is, however, insufficient for producing perceptual thumbnails, since the pictures may contain spatially varying blurs. For example, the out-of-focus regions may appear different blur strength at different depth. This raises the demands for local blur estimation. Although there are lots of existing work on spatially varying blur determination [48], [49], [50], most of them rely on solving optimization problems, which are usually time-consuming and inconvenient, thus are not suitable for efficiently generating perceptual thumbnails. We now introduce two techniques for roughly determining a local blur strength map from a high-resolution image, which were proposed in [5] and [9], respectively.

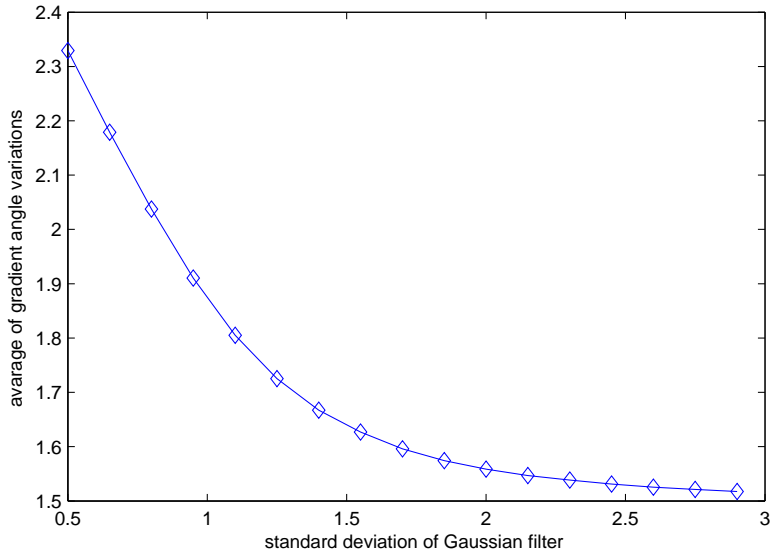


Figure 1.6: Inverse relationship of blur strength and regional variance of gradient directions.

Gradient-based blur estimation

Gradient-based blur estimation [5] relies on an important observation, i.e., the variation of a blurry edge region is much more gradual than that of a sharp edge region. Thus, the strength of regional blurriness can be quantitatively measured according to the variance of gradient angles/directions within the corresponding edge region. Specifically, the smaller the regional variance of gradient angles is, the more blurry the edge region would be. To verify this fact, we show a simulation test in Figure 1.6. In this simulation, each of the six high-resolution images were blurred by Gaussian filters with increased standard deviations. We then

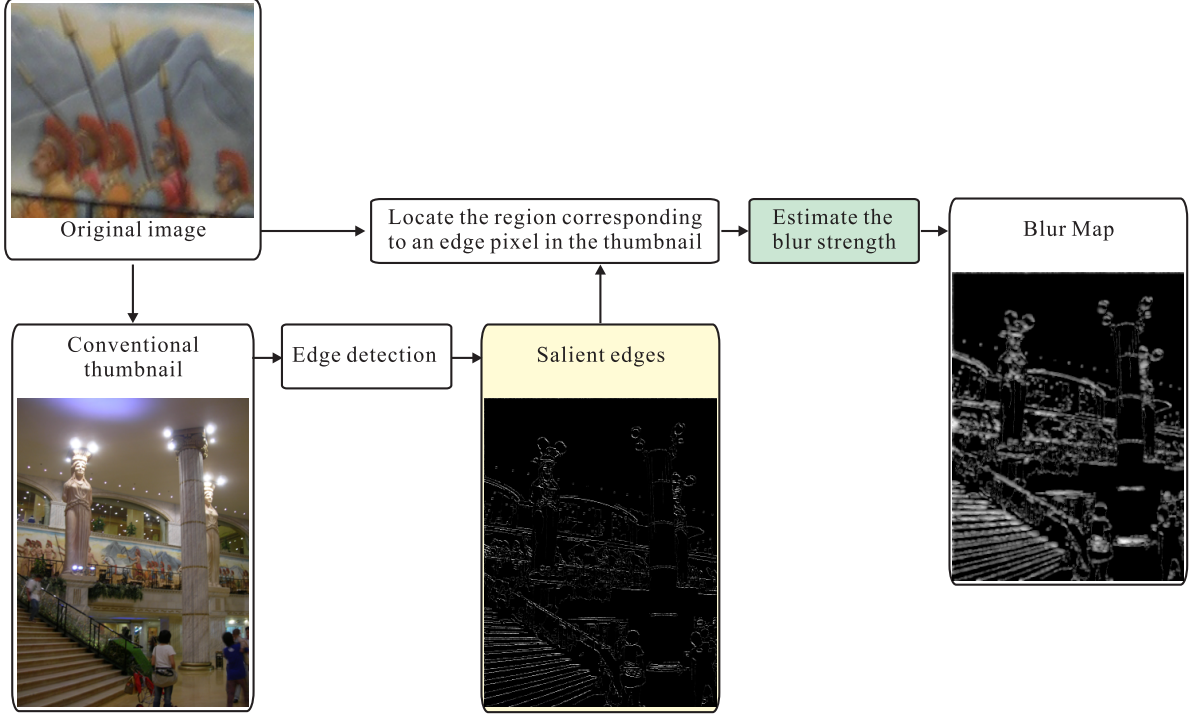


Figure 1.7: Flowchart of gradient-based blur estimation.

measured the variances of gradient directions in all edge regions. As shown in Figure 1.6, as the strength of Gaussian filters increases, the average of directional variances in the gradient field decreases significantly.

Let A_i denote the gradient angle of the i -th edge pixel, which can be obtained by

$$A_i = \arctan\left(\frac{\Delta_t(i)}{\Delta_s(i)}\right), \quad (1.5)$$

where $\Delta_t(i)$ and $\Delta_s(i)$ are the first-order differences of pixel i along two spatial dimensions. Then, the gradient-based space-varying blur metric can be defined as

$$B_i = \alpha \exp(-\beta \text{var}(A_i)^\tau), \quad (1.6)$$

where $\text{var}(\cdot)$ is the variance operator and returns the direction variance within the neighborhood of pixel i . Parameters α , β and τ control the influence of local gradient directional variance to the estimated blur strength. With this equation, the estimated blur strength is increasing with respect to the standard deviation of the Gaussian filter, as shown in Figure 1.9(a).

In the context of perceptual thumbnail generation, there is no need to estimate the blur metric for the entire image at the original high-resolution. In fact, we need only to partially measure the blur strength in the low-resolution thumbnail image. Specifically, we already know that the blur around edge regions is visually much more noticeable and important to the viewers than other regions [5], even the entire image is very blurry. Hence, to speed up the computation, gradient-based blur estimation and highlight can be performed

only around the edge regions in the thumbnail image by referring to its original version at the high resolution. As a result, as illustrated in Figure 1.7, gradient-based blur estimation is a three-step process. First, edge detection is performed on the conventional thumbnail to get salient edge pixels. Second, for each edge pixel in the thumbnail, we find its corresponding region at the original high-resolution picture. This small region defines the pixel neighborhood that is used to evaluate the gradient angle variance of current edge pixel. Finally, the blur metric is computed according to Equation (1.6). By this way, we are able to get a blur strength map for all edge pixels in the thumbnail image. See Figure 1.7 for an example.

Scale-space-based blur estimation

Scale-space-based blur estimation [9] also generates a space-varying blur map. Its basic idea, in contrast to gradient-based estimation, is to smooth the conventional thumbnail using various Gaussian kernels with different scales, and then to find the best filter scale such that the smoothed region in the filtered thumbnail image is most similar to the corresponding region in the high-resolution image. The algorithmic flow of scale-space-based blur estimation is illustrated in Figure 1.8. Note that, to generate a space-varying blur map, such filter scale matching is performed for the entire thumbnail image. Similar to gradient-based blur estimation, this method does not differentiate motion blur and out-of-focus blur either, and just estimates the pixel-level blur metric. But different to gradient-based blur estimation, this scale-space method estimates the blur strength of all pixels in the thumbnail image.

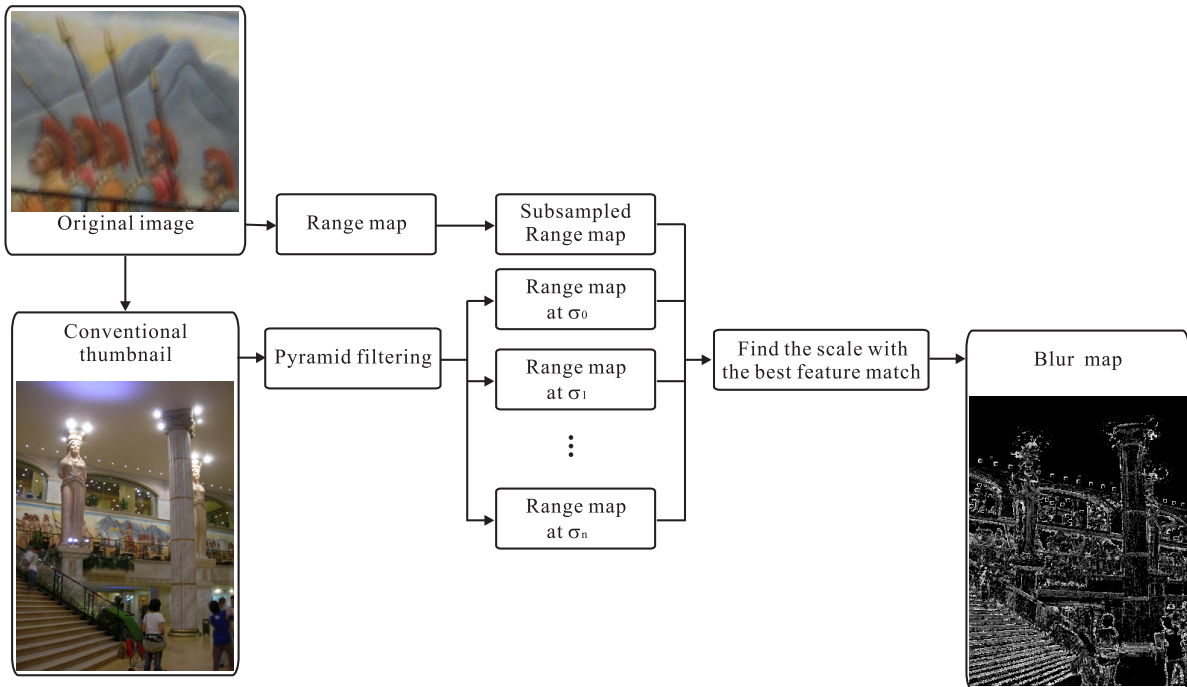


Figure 1.8: Flowchart of scale-space-based blur estimation.

In more detail, the conventional thumbnail y is blurred by a series of Gaussian kernels g with increasing scales $\{\sigma_j\}$, generating an indexed set of filtered thumbnails f_j , given by

$$f_j = g(\sigma_j) * y, \quad (1.7)$$

where $g(\cdot)$ represents Gaussian filter. As shown in Figure 1.8, for each blurred thumbnail, a local feature is extracted at each pixel and is compared to the features extracted from the high-resolution image. Here, the local feature of a pixel is defined as the maximum absolute difference between the appearances of the pixel and its surrounding eight neighbors. This generates a series of range maps $\{r_j\}$ [9], where j is the index of evaluated Gaussian filter scales. Similarly, a range map for the high-resolution image is generated and subsampled to the thumbnail scale by further taking the maximum range value in a high-resolution neighborhood conforming to the subsampling factor. Specifically, denote the subsampled range map to be r_o . The blur map index at pixel i can then be computed as

$$m_i = \min_j \{j \mid r_j(i) \leq \gamma r_o(i)\}, \quad (1.8)$$

where the parameter γ controls the amount of highlighted blur in thumbnails. Empirically, besides the conventional thumbnail, ten additional scales were used in our experiments, starting from $\sigma_1 = 0.5$ and ending at $\sigma_{11} = 2.4$ with an increment of 0.2111. Note that, in Equation (1.8) the blur map returns the index of Gaussian filters evaluated. For illustration purpose, we visualize the corresponding blur scale in Figure 1.8.

1.4.2 Blur visualization

The second step of perceptual blur highlight is *faithful blur visualization*. After either gradient-based blur estimation [5] or scale-space-based blur estimation [9], the extracted space-varying blur maps control Gaussian kernels with varying scales, which are finally superimposed into the downsampled thumbnail y pixel by pixel and result in the faithfully blurred thumbnail y_b . Note that, although the actual image blur in the original resolution may not be exactly conformed to Gaussian kernels, it is empirically a reasonable and effective choice to use Gaussian filters in the blur visualization for perceptual thumbnails, as we need only a visually faithful and noticeable blur effect.

Particularly, there are two types of methods to superimpose the space-varying Gaussian blurs in thumbnails. The first method is *incremental superimposition*. For the case of gradient-based blur estimation [5], the estimated pixel-level blur metric can be used as the standard deviation of a Gaussian filter. Note that, the blur is estimated only at edge pixels of the conventional thumbnail. To get a reliable blurring effect, we diffuse the blur strength at edge pixels to their neighborhood with self-adjusted filter scales. Approximately, the blur metric for one pixel near an edge region is computed as a weighted average of blur strengths of

edge pixels nearby. The second method is *independent superimposition*. For the case of scale-space-based blur estimation [9], the estimated blur value corresponds to a specific Gaussian kernel with particular scale. Since the blur estimation is conducted at the entire thumbnail image, we can select pixel values from the blurred thumbnail directly, given by

$$y_b(i) = f_{m_i}(i), \quad (1.9)$$

where m_i is the detected index of Gaussian filters for pixel i , f_{m_i} is the smoothed neighborhood of pixel i in the thumbnail image.

Note that, both incremental and independent superimposition have respective pros and cons. For instance, we can find from Figure 1.13 and Figure 1.14, independent superimposition tends to produce artifacts in the blurred thumbnails, since there is nothing to protect the spatial coherence of blur strength by independent blur rendering; while incremental superimposition has no such problem. On the other hand, however, the exact blur strength rendered into the thumbnail image is not implicitly clear if using incremental superimposition.

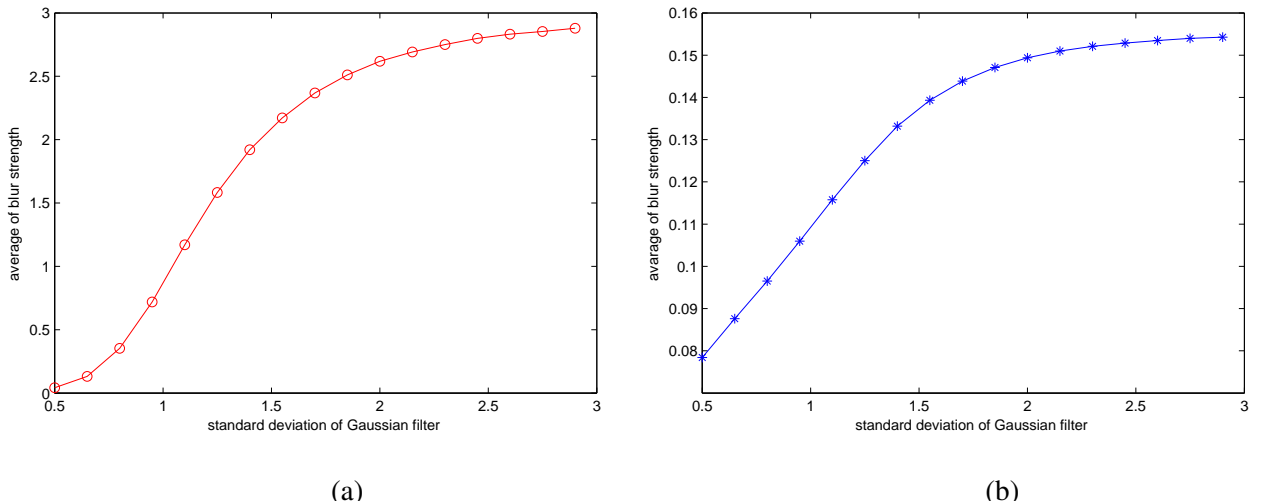


Figure 1.9: Relationship between detected blur strength and the ground truth Gaussian filter scales. (a) Gradient-based blur estimation. (b) Scale-space-based estimation.

1.4.3 Evaluation

A simulation test with uniform blur is conducted to study how the blurriness is preserved across different blur strengths. We first collect a set of six sharp high-resolution images as the test data set. Then, each high-resolution image is blurred by a series of Gaussian kernels with increasing standard deviations. The conventional thumbnails that match different blur strengths are prepared as well. Finally, the average blur strength, by gradient-based blur estimation and scale-space-based blur estimation, is obtained for each

image.

Figure 1.9 shows the results of the average of the estimated blur standard deviation for the data set. For gradient-based blur estimation, the estimated blur standard deviation is the computed blur metric. For scale-space-based blur estimation, we retrieve the standard deviation of matched filter according to the estimated index of tested Gaussian kernels. From Figure 1.9, we can see that both methods can reasonably generate increased blur standard deviations as the blur gets more severe. In addition, the estimated blur standard deviation increases rapidly for small blur scales, and becomes saturated for large blur scales, for both blur estimation methods.

1.5 Highlight Noise in Thumbnails

To highlight image noise in the thumbnail also involves two major steps, i.e., estimating the noise in a high-resolution image, and visualizing the noise in the image thumbnail.

1.5.1 Noise estimation

Traditional image denoising [51], [43], [44] aims to reconstruct a noise-free image from the noisy original image. It is critical to have an accurate estimate of noise, otherwise the recovered image is still degraded. In perceptual thumbnail generation, the goal is to visualize noise and the exact precise form of the noise is not necessary for displaying noise in thumbnails. This relieves the requirement for noise estimation in two aspects. Firstly, some prior knowledge about noise distribution can be exploited. Secondly, fast and inexact noise estimation methods can be used, such as [5] and [9].

Region-based noise estimation

Image noise, as introduced in Section 1.3, is generated by image sensors during image acquisition. It is distributed over the entire image irrespective of the image content. However, image noise is more visually apparent to the viewer in intensity-uniform regions than texture-intensive regions. It is because image noise is high frequency signal. Texture regions also have lots of high frequency details, therefore it is usually difficult to differentiate image noise from high frequency texture details. Uniform regions, on the contrary, contain much less details, and hence the high-frequency information in uniform regions are mainly from image noise. Taking this prior knowledge, a region-based noise estimation is developed in [5]. Its basic idea is to detect noise in a small uniform region in the high-resolution image, and then to synthesize a noise map in the thumbnail resolution based on the estimated noise region. Figure 1.10 illustrates the procedure.

Region-based noise estimation starts with the conventional thumbnail y and divides it into non-overlapped regions $\{\Omega_k(y)\}$. The most uniform region $\Omega_u(y)$ is selected as the one with the minimum

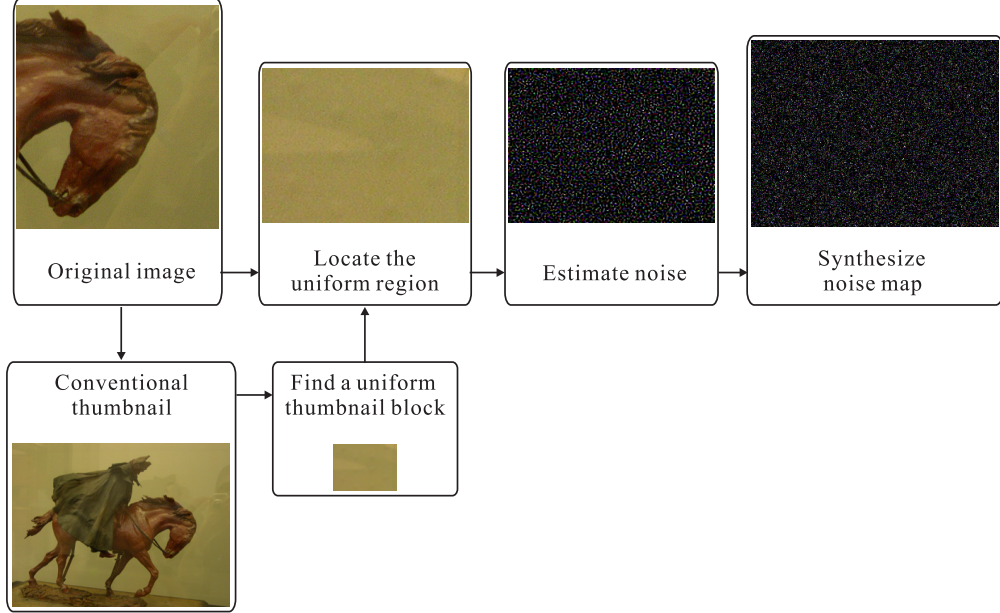


Figure 1.10: Region-based noise estimation.

intensity variance, which is given by

$$\Omega_u(y) = \min_k \{k | \text{var}(\Omega_k(y))\}. \quad (1.10)$$

The uniform region $\Omega_u(x)$ in the high-resolution image can then be determined from $\Omega_u(y)$ via upsampling. To estimate the noise in $\Omega_u(x)$, a wavelet-based soft thresholding [51] is used. It first obtains empirical wavelet coefficients c_l by pyramid filtering the noisy region $\Omega_u(x)$. Next, the soft thresholding nonlinearity is applied to the empirical wavelet coefficients respectively, given by

$$\hat{c}_l = \text{sgn}(c_l)(|c_l| - t)_+, \quad (1.11)$$

where the operator $(a)_+ = a$ if $a \geq 0$ and $(a)_+ = 0$ if $a < 0$. The threshold t is specially chosen as $t = 1.6\sigma_l \sqrt{2 \log(N)/N}$, where N is the number of pixels in the noisy uniform region $\Omega_u(x)$. The noise standard deviation is estimated as $\sigma_l = c_m / 0.6745$, where c_m is the median absolute value of the normalized wavelet coefficients. Finally, the noise-free uniform region $\Omega_u(\hat{x})$ is recovered by inverting the pyramid filtering and the noise region is determined with

$$n_u(x) = \Omega_u(x) - \Omega_u(\hat{x}). \quad (1.12)$$

Note that the estimated noise region $n_u(x)$ may not be in the thumbnail resolution. Hence, a noise map $n(x)$ in the thumbnail resolution needs to be created. As noise distributes uniformly in the high-resolution image, we can use a simple yet efficient method to obtain $n(x)$. For each pixel in $n(x)$, we randomly select its value from the estimated noise region $n_u(x)$. Although the resulted noise map $n(x)$ may not have exact match in the high-resolution image, it offers the viewer a quite similar visual experience.

Multirate-based noise estimation

Samadani et al. [4] also based their noise estimation on the wavelet-based soft thresholding [51]. Instead of a full wavelet transform, they only used the single high-pass filtered signal to generate the noise. The single high-pass filtered signal is determined by

$$x_h = x - g(\sigma) * x, \quad (1.13)$$

where $g(\sigma)$ is a Gaussian filter with standard variation $\sigma = 1$. The soft threshold nonlinearity, as defined in Equation (1.11), is applied to the filtered signal. Then the noise map is given by

$$\rho(i) = \begin{cases} x_h(i), & \text{if } x_h(i) < \tau, \\ \tau, & \text{otherwise.} \end{cases} \quad (1.14)$$

Note that differing from region-based noise estimation, the threshold τ is estimated from x_h without performing wavelet transform. In the current discussion, the noise estimate ρ is at the high resolution of the original image. According to [52], subsampling the noise estimate ρ by a scaling factor t generates the noise map n at the thumbnail resolution with the same standard deviation. Therefore the noise map n can be computed as

$$n(i) = \rho(ki). \quad (1.15)$$

In this noise estimation algorithm, estimating ρ can be rather slow due to the high resolution of the original image. In their subsequent work [9], Samadani et al. developed a fast algorithm by exchanging the order of subsampling and noise generation. More specifically, they used multirate signal transformations [52] to estimate the noise at the low thumbnail resolution. Multirate-based noise estimation is feasible thanks to the observation that there are enough pixels at the thumbnail resolution for the determination of the noise standard deviation. In addition, the soft threshold nonlinearity commutes with the subsampling operator. Due to these two facts, subsampling can be applied to the high-resolution image and the noise estimate is performed on the subsampled low resolution image. Note that the threshold τ is estimated from the low resolution image subsampled from the high resolution image. Figure 1.11 illustrates the process of multirate-based noise estimation. Readers are referred to [9] for a more detailed analysis on multirate-based noise estimation.

1.5.2 Noise Visualization

To visualize noise is rather simple. As the noise is assumed to be additive to the ideal signal, the noise-preserved thumbnail is formed by adding the estimated noise map n to the thumbnail. Considering image blur, the noise visualization is performed after blur visualization, i.e.,

$$y_n(i) = y_b(i) + mag * n(i), \quad (1.16)$$

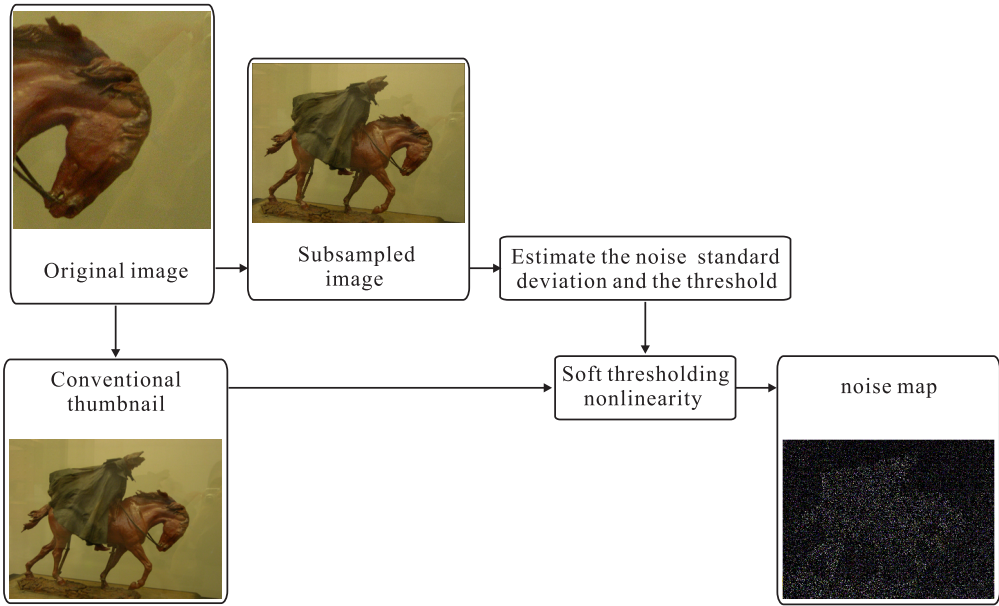


Figure 1.11: Region-based noise estimation.

where the parameter mag controls the strength of noise to be visualized.

1.5.3 Evaluation

A simulation using a noise image is conducted to evaluate the performance of the two noise estimation methods. To roughly simulate the observed noise in photographs [53], the noise image is generated by adding a Gaussian noise with the standard deviation $\sigma = 10/255 = 0.392$ to a gray image with constant values. The simulation downsamples the 2048×1536 noise image (one patch is shown in Figure 1.12) by different subsampling factors. At each subsampling scale, a 100×100 region is cut for illustration. It is obvious that increasing the subsampling scale reduces the strength of noise gradually. In the thumbnail of a resolution 205×154 , the noise is almost invisible. The two noise estimation methods are applied at each downsampling scale to estimate the noise map. Figure 1.12 shows the results of the standard deviations for the estimated noise maps with respect to the subsampling factors. The conventional thumbnail has a decreased standard deviation. The decreasing slope verifies the observation that the larger the subsampling factor is, the less noisy the thumbnail appears. Both noise estimation methods, on the other hand, have near-horizontal lines and quite close to the ideal curve. The results tell us that the two methods are able to preserve the noise standard deviations faithfully across scale.

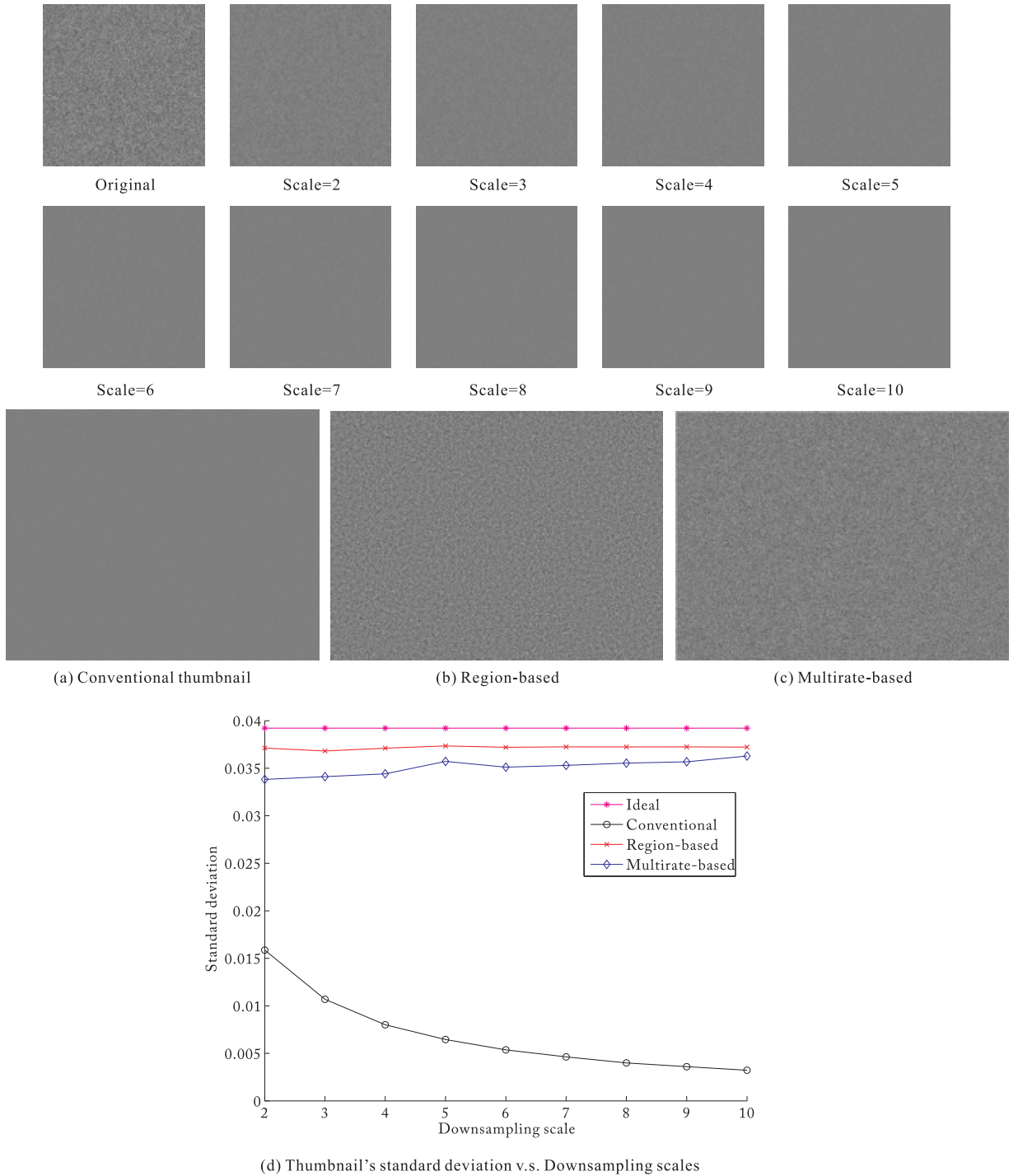


Figure 1.12: Evaluation of noise estimation. The top two rows show a 100×100 region in the original noise image and its conventional thumbnails at different downsampling scales. (a) the conventional thumbnail at scale=10. (b) the corresponding region-based thumbnail. (c) the corresponding multirate-based thumbnail. (d) the curves of standard deviation of pixel intensities against the downsampling scales.

1.6 Results and Discussion

In this section, we present some experimental results and comparisons of perceptual thumbnail generation with the ability of highlighting blur and noise, if any. Note that, all results reported in this section were produced using the same set of parameters: $\alpha = 1$, $\beta = 3.0$, $\tau = 2.0$, $\gamma = 1.5$.

We first report the experimental results on blur highlighting. Note a good blur highlighting algorithm should be able to reflect blur when there exists blur, and not to introduce obvious blur when the picture is sharp. Figure 1.13 demonstrates a blurry picture suffered to camera shake. The conventional thumbnail (at a resolution of 423×317) appears rather clear and sharp, although blowups in the original high-resolution image (2816×2112) look blurry. Both gradient-based and scale-space-based blur estimation can reflect blur in the modulated thumbnails. We also visualize the corresponding blur maps. It can be seen that both methods take effects around edge regions. The difference is that gradient-based method visualizes blur around salient edges only, while scale-space-based method is effective in most edges, including weak edges. In terms of visual experience, scale-space-based method introduces larger blur that is more visible to viewers, however, its rendered blur somehow appears in blocky artifacts.

Now that the existing blur highlighting methods are effective for blurry pictures, we exploit their performance in the case of sharp pictures, for which the methods are expected to introduce as small blur as possible. Look at Figure 1.14. The two high-resolution pictures (2048×1536) are shot without motion blur or camera shake. We can see in the image blowup that the edges are rather strong and sharp. Hence, the perceptual thumbnail at a resolution of 308×231 should look similar to the conventional thumbnail, which is also sharp and clear. A close inspection to the thumbnails in Figures 1.14(c),(d),(f) and (g) reveals that either gradient-based method or scale-space-based method will introduce some blur in the resulted thumbnails. From side-by-side comparison, we find that gradient-based method suffers less to the unexpected blur, and scale-space-based method may introduce obvious distracting blur in some regions.

We now report the experimental results for noise highlighting. Similar to the requirements of blur highlighting methods, a good noise highlighting method shall be able to visualize image noise for noisy images, and not to introduce apparent noise for noise-free images. Figure 1.15 compare the conventional thumbnail and the perceptual thumbnail from region-based noise estimation and multirate-based noise estimation. The two high-resolution images (of a size of 2272×1704 and 2048×1536) suffer from severe noise, however, we cannot detect such noise by viewing their conventional thumbnails. On the contrary, the two noise estimation methods are able to generate thumbnails that reflect noise in a similar way to the original high-resolution images.

In Figure 1.16, we perform noise estimation for a noise-free high-resolution image (2048×1536). The perceptual thumbnail should be similar to the conventional thumbnail which looks clean. Let us compare the

results visually. The thumbnail from region-based noise estimation is almost the same to the conventional thumbnail. The thumbnail from multirate-based noise estimation has details enhanced in texture-intensive regions. In this example, we use the parameter $mag = 2$ in Equation (1.16) for both noise estimation methods. To lower the detail enhancement, we may use a smaller value for the parameter mag .

Finally, we show an example that combines both blur highlighting and noise highlighting. In this example, the high-resolution image (2048×1536) suffers to image blur and noise that take effect in the entire image. The second row in Figure 1.17 demonstrates the thumbnails generated by using bilinear, bicubic and lanczos filtering methods. All the three thumbnails appear rather clean and clear, by viewing which users cannot tell that the high-resolution image is noisy and blurry. We then show the thumbnails by adding blur only according to gradient-based and scale-space-based blur estimation methods. Comparing the resulted thumbnails with the conventional one, image blur is reflected in the resulted thumbnails. The final thumbnails are generated by superimposing the estimated noise. Note how the final thumbnails (Figures 1.17(h) and (k)) reflect the blur and noise as the high-resolution image does.

1.7 Conclusion

This chapter introduces perceptual thumbnail generation, a practical problem available in digital photography, image browsing, image searching, web-based applications. Differing from conventional image thumbnail, perceptual thumbnail offers users the capability of inspecting the image quality at the small thumbnail resolution. Perceptual thumbnail serves in an intuitive way by displaying the perception-related visual cues in the thumbnail. Consequently, users can judge the image quality by viewing the thumbnail alone.

Perceptual thumbnail generation is still a rather new problem in the field of computer vision and media computing. Existing methods mainly focus on two low-level visual cues, i.e., blur and noise. Although blur and noise estimation and removal have been extensively studied. The goal of most techniques is to recover the blur kernel and noise model and in turn to reconstruct the ideal image. Perceptual thumbnail dose not have such strict requirements for blur and noise estimation. A rough and fast estimation is sufficient and necessary for such application. Existing techniques on perceptual thumbnail generation exploit how to assess the local spatial-varying blur strength and the noise in a fast way.

One potential future task for perceptual thumbnail generation is to highlight other visual cues, like the red-eye effect. For the red-eye effect, there are lots of works in the literature for red-eye detecting and removal [36], [37]. The difficulty lies in that visualizing red eyes in the thumbnail is not as straightforward as highlighting blur and noise. Superimposing the detected red eyes with the thumbnail may result in a weird preview. To highlight red eyes in the thumbnail, a possible solution is to mark its region in the thumbnail. For example, we may draw a red ellipse around the defected eyes. For image bloom, a similar problem

exists, i.e., how to visualize it effectively.



Figure 1.13: Highlighting blur in the thumbnail when the original picture is blurred. (a) The conventional thumbnail at a resolution of 423×317 . (b) Two blowups in the original high resolution image (2816×2112). (c) shows the perceptual thumbnail by the gradient-based blur estimation, and (d) is its corresponding blur map. (e) shows the perceptual thumbnail by the scale-space-based blur estimation, and (f) is its corresponding blur map.

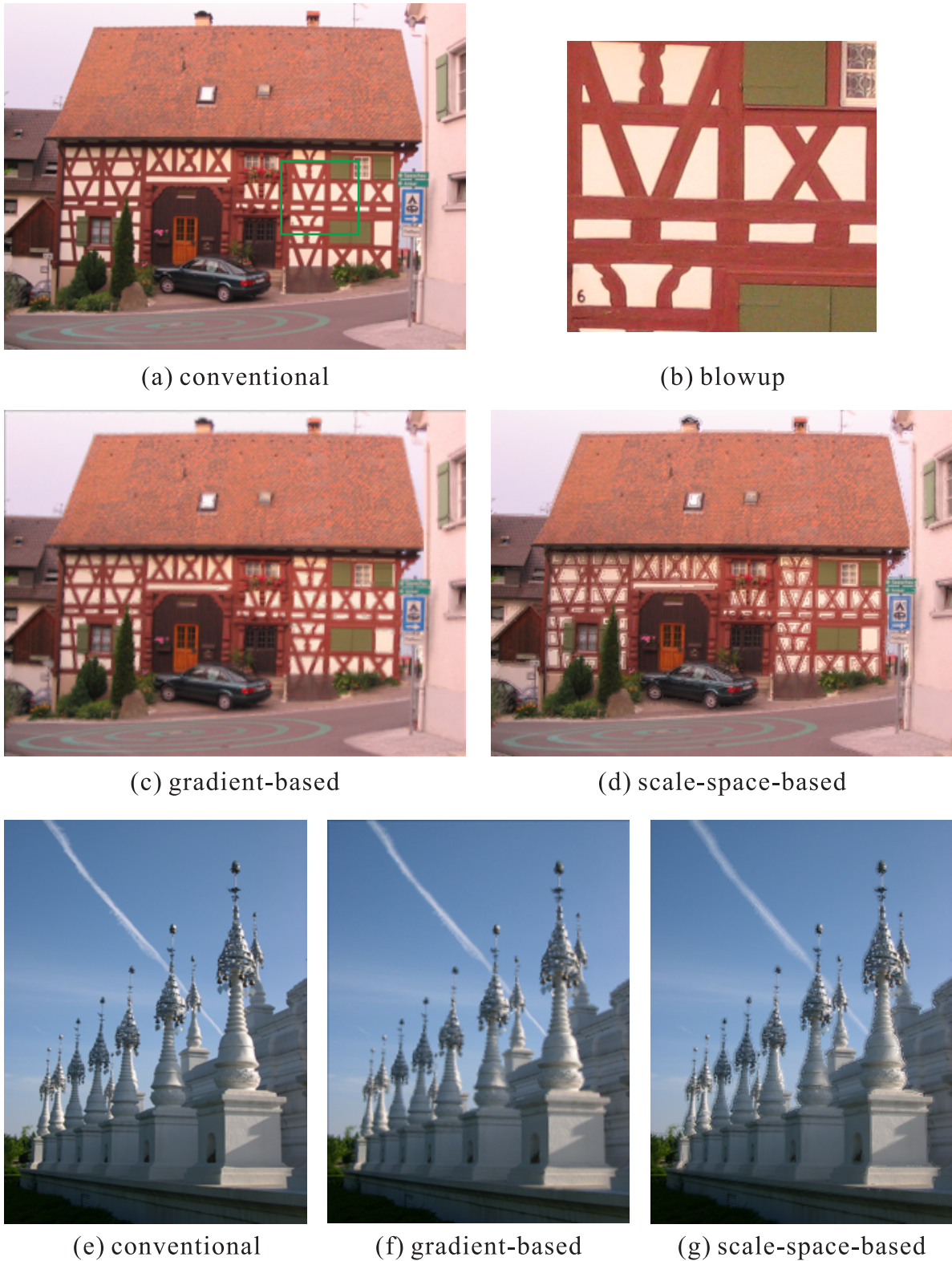


Figure 1.14: Highlighting blur in the thumbnail when the original picture is clear. (a) The conventional thumbnail at a resolution of 308×231 . (b) One blowup in the original high resolution image (2048×1536). (c) and (d) are the perceptual thumbnails by the gradient-based blur estimation and the scale-space-based blur estimation, respectively. (e) is another conventional thumbnail. (f) and (g) are the perceptual thumbnails by the gradient-based blur estimation and the scale-space-based blur estimation, respectively.



Figure 1.15: Highlighting noise in the thumbnail. Two high-resolution noisy images are shown in (a) and (f). (b) and (g) give two blowups in the image. The conventional thumbnail, thumbnails from region-based method and multirate-based method are shown in (c) and (h), (d) and (i), (e) and (j), respectively.

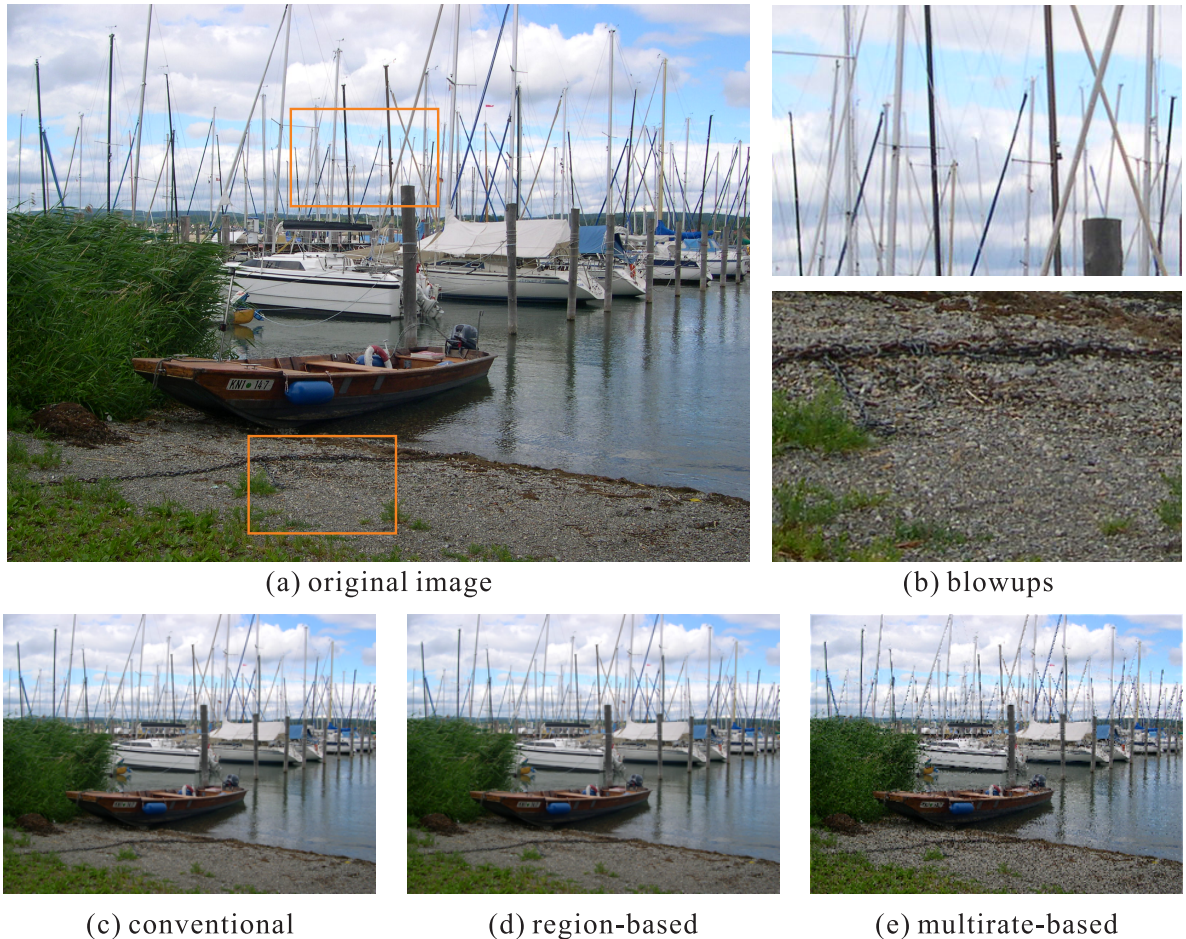


Figure 1.16: Highlighting noise in the thumbnail. (a) A high-resolution noise-free image. (b) shows two blowups of the original image. (c) The conventional thumbnail. (d) The thumbnail from region-based noise estimation method. (e) The thumbnail from multirate-based noise estimation method.



Figure 1.17: Highlighting blur and noise in the thumbnail. (a) The high-resolution image has both blur and noise. (b) shows two blowups. Conventional thumbnails generated using three common filtering methods are shown in (c) to (e). Then gradient-based and scale-space-based blur estimation methods are performed to get the blur maps in (f) and (i), and the blur-enhanced thumbnails in (g) and (j). The final thumbnails by adding noise are shown in (h) and (k), respectively.

Bibliography

- [1] C. Burton, J. Johnston, and E. Sonenberg, “Case study: an empirical investigation of thumbnail image recognition,” in *Proceedings of Information Visualization*, pp. 115–121, 1995.
- [2] K. Berkner, E. Schwartz, , and C. Marle, “Smartnails: Display- and image-dependent thumbnails,” in *Proceedings of SPIE Document Recognition and Retrieval XI*, pp. 54–65, 2003.
- [3] A. Woodruff, A. Faulring, R. Rosenholtz, J. Morrison, and P. Pirolli, “Using thumbnails to search the web,” in *Proceedings of The ACM Conference on Human Factors in Computing Systems*, pp. 198–205, 2001.
- [4] R. Samadani, S. H. Lim, and D. Tretter, “Representative image thumbnails for good browsing,” in *Proceedings of the IEEE International Conference on Image Processing*, vol. 2, pp. 193–196, 2007.
- [5] L. Wan, W. Feng, Z. C. Lin, T. T. Wong, and Z. Q. Liu, “Perceptual image preview,” *Multimedia Systems*, vol. 14, no. 4, pp. 195–204, 2008.
- [6] W. Burger and M. J. Burge, *Principles of digital image processing: core algorithms*. Springer, 2009.
- [7] A. Muñoz, T. Blu, and M. Unser, “Least-squares image resizing using finite differences,” *IEEE Transactions on Image Processing*, vol. 10, no. 9, pp. 1365–1378, 2001.
- [8] L. Q. Chen, X. Xie, X. Fan, W. Y. Ma, H. J. Zhang, and H. Q. Zhou, “A visual attention model for adapting images on small displays,” *ACM Multimedia Systems Journal*, vol. 9, no. 4, pp. 353–364, 2003.
- [9] R. Samadani, T. A. Mauer, D. M. Berfanger, and J. H. Clark, “Image thumbnails that represent blur and noise,” *IEEE Transactions on Image Processing*, vol. 19, no. 2, pp. 363–373, 2010.
- [10] R. G. Keys, “Cubic convolution interpolation for digital image processing,” *IEEE Transaction on Acoustics, Speech, and Signal Processing*, vol. 29, pp. 1153–1160, 1981.
- [11] M. Unser, “Splines: a perfect fit for signal and image processing,” *IEEE Transaction on Signal Processing*, vol. 16, pp. 22–38, 1999.
- [12] E. H. W. Meijering, W. J. Niessen, and M. A. Viergever, “Piecewise polynomial kernels for image interpolation: a generalization of cubic convolution,” in *Proceedings of IEEE International Conference of Image Processing*, pp. 25–28, 1999.
- [13] X. Li, *Edge directed statistical inference with applications to image processing*. PhD thesis, Princeton University, 2000.

- [14] B. Suh, H. Ling, B. B. Bederson, and D. W. Jacobs, “Automatic thumbnail cropping and its effectiveness,” in *Proceedings of the 16th Annual ACM Symposium on User Interface Software and Technology*, pp. 95–104, 2003.
- [15] S. Avidan and A. Shamir, “Seam carving for content-aware image resizing,” *ACM Transaction on Graphics*, vol. 26, no. 3, pp. 10:1–10:9, 2007.
- [16] Y.-S. Wang, C.-L. Tai, O. Sorkine, and T.-Y. Lee, “Optimized scale-and-stretch for image resizing,” *ACM Transactions on Graphics*, vol. 27, pp. 118:1–118:8, 2008.
- [17] P. Thévenaz, T. Blu, and M. Unser, *Image interpolation and resampling*. New York: Academic, 2000.
- [18] D. P. Mitchell and A. N. Netravali, “Reconstruction filters in computer computer graphics,” in *Computer Graphics, (Proceedings of SIGGRAPH 88)*, vol. 22, pp. 221–228, 1988.
- [19] N. Greene and P. Heckbert, “Creating raster omnimax images from multiple perspective views using the elliptical weighted average filter,” *IEEE Computer Graphics and Applications*, vol. 6, no. 6, pp. 21–27, 1986.
- [20] P. Heckbert, “Fundamentals of texture mapping and image warping,” Master’s thesis, U. C. Berkeley, 1989.
- [21] J. McCormack, R. Perry, K. I. Farkas, and N. P. Jouppi, “Feline: Fast elliptical lines for anisotropic texture mapping,” in *Proceedings of the 26th Annual Conference on Computer Graphics and Interactive Techniques*, pp. 243–250, 1999.
- [22] X. Li and M. Orchard, “New edge-directed interpolation,” *IEEE Transactions on Image Processing*, vol. 10, pp. 1521–1527, 2001.
- [23] D. Muresan and T. Parks, “Adaptively quadratic (aqua) image interpolation,” *IEEE Transactions on Image Processing*, vol. 13, no. 5, pp. 690–698, 2004.
- [24] L. Zhang and X. Wu, “An edge-guided image interpolation algorithm via directional filtering and data fusion,” *IEEE Transactions on Image Processing*, vol. 15, pp. 2226–2238, 2006.
- [25] R. Fattal, “Image upsampling via imposed edge statistics,” *ACM Transactions on Graphics*, vol. 26, pp. 95:1–95:8, 2007.
- [26] V. R. Setlur, *Optimizing computer imagery for more effective visual communication*. PhD thesis, Northwestern University, 2005.
- [27] Y. Pritch, E. Kav-venaki, and S. Peleg, “Shift-map image editing,” in *Proceedings of the International Conference on Computer Vision*, pp. 151–158, 2009.
- [28] P. Kráhenbühl, M. Lang, A. Hornung, and M. Gross, “A system for retargeting of streaming video,” *ACM Transactions on Graphics*, vol. 28, pp. 126:1–126:10, 2009.
- [29] M. Rubinstein, A. Shamir, and S. Avidan, “Multi-operator media retargeting,” *ACM Transactions on Graphics*, vol. 28, pp. 23:1–23:11, 2009.
- [30] M. Rubinstein, D. Gutierrez, O. Sorkine, and A. Shamir, “A comparative study of image retargeting,” *ACM Transactions on Graphics*, vol. 29, pp. 160:1–160:10, 2010.

- [31] H. Lam and P. Baudisch, “Summary thumbnails: readable overviews for small screen web browsers,” in *Proceedings of the SIGCHI conference on Human factors in computing systems*, pp. 681–690, 2005.
- [32] A. Cockburn, C. Gutwin, and J. Alexander, “Faster document navigation with space-filling thumbnails,” in *Proceedings of the SIGCHI conference on Human Factors in computing systems*, pp. 1–10, 2006.
- [33] S. Baluja, “Browsing on small screens: recasting web-page segmentation into an efficient machine learning framework,” in *Proceedings of the 15th international conference on World Wide Web*, pp. 33–42, 2006.
- [34] A. Wrotniak, “Noise in digital cameras.” <http://www.wrotniak.net/photo/tech/noise.html>, 2008.
- [35] Y. Ke, X. Tang, and F. Jing, “The design of high-level features for photo quality assessment,” in *Proceedings of the IEEE Conference on Computer Vision and Pattern Recognition*, vol. 1, pp. 419–426, 2006.
- [36] L. Zhang, Y. Sun, M. Li, and H. Zhang, “Automated red-eye detection and correction in digital photographs,” in *Proceedings of the International Conference on Image Processing*, vol. 4, pp. 2363–2366, 2004.
- [37] F. Volken, J. Terrier, and P. Vandewalle, “Automatic red-eye removal based on sclera and skin tone detection,” in *Proceedings of IS&T Third European Conference on Color in Graphics, Imaging and Vision*, pp. 359–364, 2006.
- [38] N. El-Yamany, *Faithful quality representation of high-resolution images at low resolutions*. PhD thesis, Southern Methodist University, 2010.
- [39] M. Trentacoste, R. Mantiuk, and W. Heidrich, “Quality-preserving image downsizing,” in *ACM SIGGRAPH 2010 Posters*, SIGGRAPH ’10, p. 74, 2010.
- [40] D. Kundur and D. Hatzinakos, “Blind image deconvolution,” *IEEE Signal Processing Magazine*, pp. 43–64, 1996.
- [41] Q. Shan, J. Jia, and A. Agarwala, “High-quality motion deblurring from a single image,” *ACM Transactions on Graphics*, vol. 27, pp. 73:1–73:10, 2008.
- [42] N. Joshi, C. L. Zitnick, R. Szeliski, and D. J. Kriegman, “Image deblurring and denoising using color priors,” in *Proceedings of the IEEE Conference on Computer Vision and Pattern Recognition*, pp. 1550–1557, 2009.
- [43] A. S. Wilsky, “Multiresolution markov models for signal and image processing,” *Proceedings of the IEEE*, vol. 90, no. 8, pp. 1396–1458, 2002.
- [44] M. Zhang and B. K. Gunturk, “Multiresolution bilateral filtering for image denoising,” *IEEE Transactions on Image Processing*, vol. 17, pp. 2324–2333, 2008.
- [45] P. Marziliano, F. Dufaux, S. Winkler, and T. Ebrahimi, “A no-reference perceptual blur metric,” in *Proceedings of the International Conference on Image Processing*, vol. 3, pp. 57–60, 2002.
- [46] J. Caviedes and F. Oberti, “A new sharpness metric based on local kurtosis, edge and energy information,” *Signal Processing: Image Communication*, vol. 19, no. 2, pp. 147–161, 2004.
- [47] R. Ferzli and L. Karam, “No-reference objective wavelet based noise immune image sharpness metric,” in *Proceedings of the IEEE International Conference on Image Processing*, vol. 1, pp. 405–408, 2005.

- [48] M. C. Chiang and T. E. Boult, “Local blur estimation and super-resolution,” in *Proceedings of the 1997 Conference on Computer Vision and Pattern Recognition*, pp. 821–826, 1997.
- [49] J. H. Elder and S. W. Zucker, “Local scale control for edge detection and blur estimation,” *IEEE Transaction on Pattern Analysis and Machine Intelligence*, vol. 20, no. 7, pp. 699–717, 1998.
- [50] S. Bae and F. Durand, “Defocus magnification,” in *Computer Graphics Forum*, vol. 25, pp. 571–579, 2007.
- [51] D. L. Donoho, “De-noising by soft-thresholding,” *IEEE Transactions on Information Theory*, vol. 41, no. 3, pp. 613–627, 1995.
- [52] P. Vaidyanathan, *Multirate Systems and Filter Banks*. Upper Saddle River, NJ, USA: Prentice Hall Signal Processing Series, 1993.
- [53] S. H. Lim, “Characterization of noise in digital photographs for image processing,” in *Proceedings of SPIE*, vol. 6069, pp. 219–228, 2006.